Transient Solar Oscillations Driven by Primordial Black Holes

Michael Kesden and Shravan Hanasoge

Phys. Rev. Lett. **107**, 111101 — Published 8 September 2011

DOI: 10.1103/PhysRevLett.107.111101

Transient solar oscillations driven by primordial black holes

Michael Kesden[1,*] and Shravan Hanasoge[2,3,†]

[1] *Center for Cosmology and Particle Physics, Department of Physics, New York University, New York, New York 10003*

[2] *Department of Geosciences, Princeton University, Princeton, New Jersey 08544*

[3] *Max-Planck-Institut für Sonnensystemforschung, Max-Planck-Straβe 2, 37191 Katlenburg-Lindau, Germany*

Stars are transparent to the passage of primordial black holes (PBHs) and serve as seismic detectors for such objects. The gravitational field of a PBH squeezes a star and causes it to ring acoustically. We calculate the seismic signature of a PBH passing through the Sun. The background for this signal is the observed spectrum of solar oscillations excited by supersonic turbulence. We predict that PBHs more massive than 10^{21} g (comparable in mass to an asteroid) are detectable by existing solar observatories. The oscillations excited by PBHs peak at large scales and high frequencies, making them potentially detectable in other stars. The discovery of PBHs would have profound implications for cosmology and high-energy physics.

The existence of black holes is one of the most startling predictions of general relativity. Astronomers have discovered two populations of black holes: stellar-mass ($m_{BH} \sim 10M_\odot$) black holes that form in the collapse of massive stars and supermassive black holes ($10^6 M_\odot \lesssim m_{BH} \lesssim 10^{10} M_\odot$) that reside in galactic centers. However, general relativity allows black holes to have any mass. Black holes much less massive than a solar mass $M_\odot$ could have formed from density perturbations in the early universe. Such perturbations were created with a wide range of wavelengths and amplitudes. Galaxies slowly grew from perturbations whose amplitudes were initially very small. Density perturbations with higher initial amplitudes might have gravitationally collapsed into PBHs [1]. The mass m_{BH} of such PBHs reflects the mass contained within the particle horizon of the universe at the time they were formed. PBHs as small as the Planck mass $m_{\rm Pl} = \sqrt{\hbar c/G} \sim 10^{-5}$ g may have formed, but those with masses less than $m_{\rm evap} \simeq 5 \times 10^{14}$ g would evaporate in less than the age of the universe [2].

A density perturbation will collapse into a black hole if its self-gravity exceeds its pressure support [3, 4]. When this pressure is supplied by radiation as in the early universe, PBHs of any mass are equally likely to form if there is a flat power spectrum of primordial density perturbations (spectral index $n_s \simeq 1$) as indicated by observations of the cosmic microwave background [5]. PBH production may be greatly enhanced at a particular mass scale if the pressure were suddenly reduced, such as during the QCD phase transition [6]. The discovery of PBHs of a given mass would thus provide insight into high-energy physics at the temperature at which this mass was contained within the particle horizon.

PBHs are also of great interest to cosmology. They are collisionless and non-relativistic, making them ideal dark-matter candidates. Observational constraints on the cosmological density Ω_{BH} of PBHs depend on their mass m_{BH}. PBHs with masses slightly above the evaporation limit $m_{\rm evap}$ emit Hawking radiation, including γ-rays with a spectrum peaking around 100 MeV [7]. Observations of the extragalactic γ-ray background by the Energetic Gamma Ray Experiment Telescope (EGRET) [8] set an upper limit $\Omega_{BH} \leq 5 \times 10^{-10}$ for $m_{BH} = m_{\rm evap}$ [9]. Since the luminosity and temperature of a PBH scale as m_{BH}^{-2} and m_{BH}^{-1} respectively, it is more difficult to observe Hawking radiation from larger PBHs. PBHs of mass $m_{BH} \gtrsim 10^{17}$ g could constitute the entirety of the dark matter ($\Omega_{BH} = \Omega_{DM} \simeq 0.23$) without violating observational constraints on Hawking radiation.

Microlensing surveys constrain the abundance of more massive PBHs. If a PBH passes between an observer and a background star, that star will be gravitationally microlensed, briefly increasing its observed flux. The duration of each lensing event is proportional to the square root of the lens mass, implying that a survey with finite cadence will miss lenses that are too small. The EROS (Expérience de Recherche d'Objets Sombres) microlensing survey sets an upper bound of 8% on the fraction of the Galactic halo mass in the form of PBHs with masses in the range $0.6 \times 10^{-7} M_\odot < m_{BH} < 15 M_\odot$ [10, 11].

Collisions with Galactic stars might constrain PBHs in this permitted range 10^{17} g $\lesssim m_{BH} \lesssim 10^{26}$ g [12]. PBHs passing through a star deposit energy by dynamical friction. The fractional loss of kinetic energy $f \sim 10^{-7}(m_{BH}/10^{26}$ g) is tiny for PBHs with speeds comparable to the velocity dispersion of Galactic dark matter. PBHs will therefore pass through stars without slowing down or accreting appreciably. A 10^{20} g PBH was estimated to emit 1 keV X-rays with a luminosity of a 10^{22} erg/s when passing through a main-sequence star like our Sun [12], but most of these X-rays will thermalize and this luminosity is much less than the Sun's background X-ray luminosity $L_X \gtrsim 10^{26}$ erg/s [14].

We instead propose searching for PBHs by the distinctive oscillations they excite when passing through the Sun. This signal was considered previously but not calculated explicitly [12]. We simulate the generation and

*Electronic address: mhk10@nyu.edu

†Electronic address: hanasoge@princeton.edu

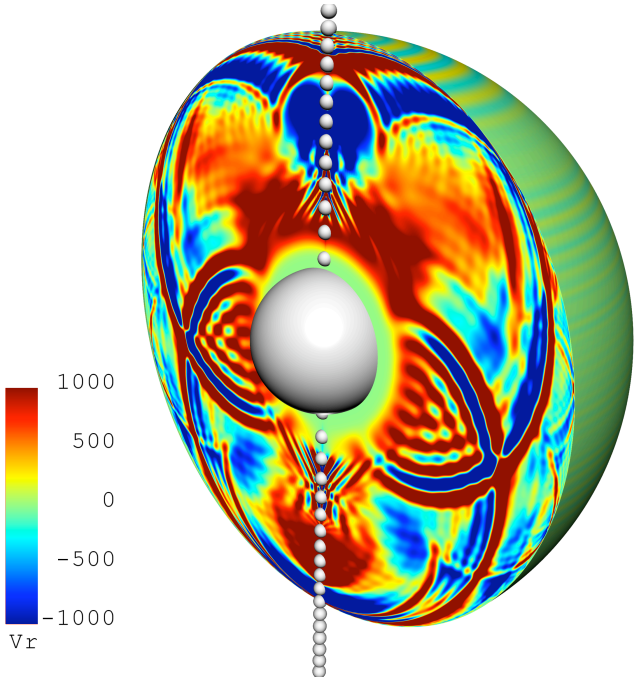

FIG. 1: Radial velocities V^{BH} induced by a 10^{-10} $M_\odot$ PBH passing through the Sun along the z axis. The grey sphere at $R < 0.24R_\odot$ is excluded from our simulations. The colors indicate the radial velocity of the fluid weighted by the square root of the density. Wave amplitudes are linearly proportional to the black-hole mass, so we may rescale our simulations to any desired value of m_{BH}.

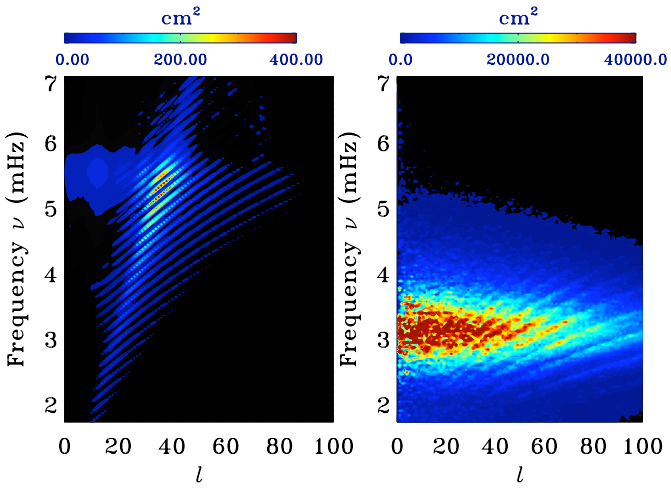

FIG. 2: Power spectra $P_l(\nu)$ of our simulated PBH signal V^{BH} (left panel) and the turbulently driven noise V^n observed by HMI (right panel) as functions of frequency ν and harmonic degree l. Each discrete ridge in both power spectra corresponds to a set of p modes with the same number of radial nodes. The signal peaks near $l \simeq 40$, $\nu \simeq 5.5$ mHz, at larger scales and higher frequencies than the noise background, helping us to distinguish them.

propagation of acoustic waves in the Sun by solving the linearized Euler equations [15] in a spherical shell with the moving PBH acting as the source. We solve these equations on a three-dimensional grid consisting of 1024 longitudinal, 512 latitudinal, and 425 radial points extending from $r/R_\odot = 0.24$ to 1.002 [16, 17]. Our simulations exclude the core ($r < 0.24$ $R_\odot$) because of the coordinate singularity at $r = 0$. We treat the PBH as a ball with radius λ comparable to our grid spacing. Although we cannot resolve the PBH's Schwarzschild radius $R_S = 1.5 \times 10^{-7}(m_{BH}/10^{21}$ g) cm, we verify convergence by repeating simulations with different values of λ. Wavefield velocities are extracted 200 km above the photosphere ($r = R_\odot$) to mimic observations.

A snapshot of one of our simulations is shown in Fig. 1. We can place the PBH's orbit (shown by grey dots) in the $x-z$ plane without loss of generality because the Sun is nearly spherically symmetric. PBH orbits in this plane are fully specified by two parameters: the energy E and angular momentum L per unit PBH mass. The PBH orbit in the simulation shown in Fig. 1 is parabolic ($E = 0$) and radial ($L = 0$). We only consider unbound orbits ($E \geq 0$) as gravitationally bound PBHs are extremely unlikely. The PBH begins at $z_i \simeq 3R_\odot$ with an inward velocity of $v_z = -\sqrt{GM_\odot/z_i}$, falls radially inwards through the Sun's center, and ends at $z_f \simeq -10R_\odot$. The total elapsed time is 8 hours, with the snapshot in Fig. 1 being taken 7.9 hours into the simulation. The radial velocity V^{BH} as a function of time t and angular position (θ, ϕ) on the Sun's surface constitutes the signal for our proposed PBH search.

Photospheric velocities are observed by measuring the Doppler shift of solar absorption lines. The Helioseismic and Magnetic Imager (HMI) [18] onboard the Solar Dynamics Observatory (SDO) currently performs such observations. The Sun has a discrete spectrum of global acoustic oscillations known as p modes because pressure provides the restoring force [15]. P modes driven by near-surface supersonic turbulence provide the dominant contribution to observed photospheric velocities, and constitute the noise background for our PBH search.

P modes can be clearly identified after the photospheric velocity field has been Fourier transformed into a function of frequency ν and decomposed into spherical harmonics $Y_{lm}(\theta, \phi)$. We show the power spectrum

$$P_l(\nu) \equiv \frac{1}{2l+1} \sum_{m=-l}^{l} |\tilde{V}_{lm}(\nu)|^2 \qquad (1)$$

of our simulated signal V^{BH} and the observed noise V^n in Fig. 2. The power spectrum in the left panel is produced from the simulation shown in Fig. 1, while the noise power spectrum in the right panel was prepared using 8 hours of publicly available HMI data [19]. The discrete ridges seen in both panels correspond to p modes with the same number of radial nodes. The power spectrum of oscillations excited by the PBH peaks at higher

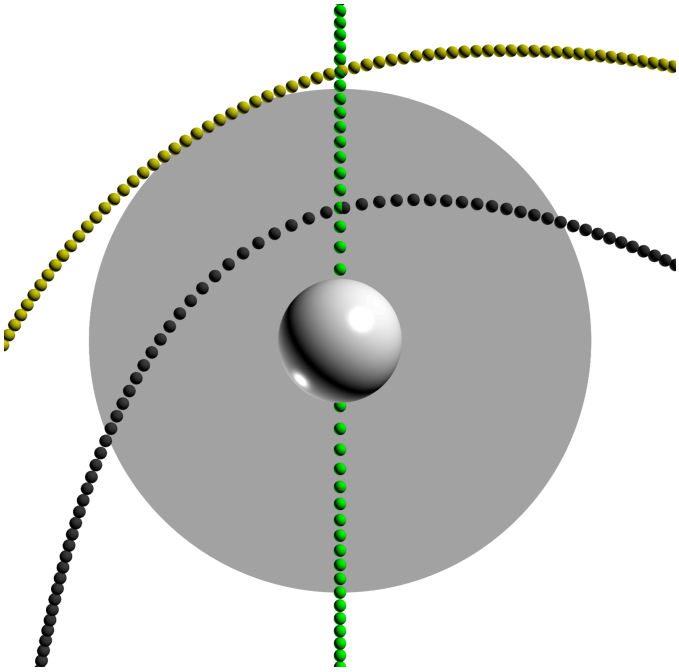

FIG. 3: Orbits of the PBHs in our simulations. The green vertical line along the z-axis shows the two radial orbits (RFF, RGC). The other two orbits are parabolic ($E = 0$). The inner black curve shows the orbit which spends the maximum amount of time within the Sun (MT), while the outer tan curve shows the orbit which skims the surface (SS).

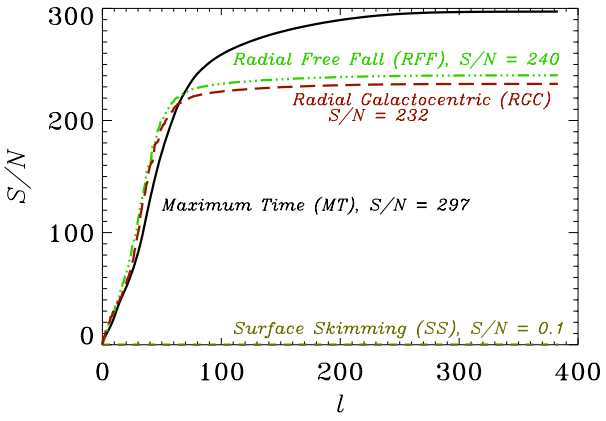

FIG. 4: Signal-to-noise ratio S/N as a function of maximum harmonic degree l for $10^{-10}M_\odot$ PBHs on the orbits shown in Fig. 3. The total S/N for each orbit is listed on each curve.

frequencies and lower harmonic degree l than the noise background driven by the Sun's natural turbulence.

This dissimilarity between the spatio-temporal dependence of the signal and noise helps us detect small signals. We treat each spherical harmonic of the noise as an independent Gaussian random variable with variance described by the observed power spectrum [15]. When data, such as the observed velocities V^{obs}, are the sum of a signal V^{BH} and a noise V^n, the likelihood that the signal is present in V^{obs} is the same as the likelihood that $V^{obs} - V^{BH}$ is a Gaussian realization of the noise in the absence of a signal [20]. This allows us to determine the signal-to-noise ratio S/N for a given event:

$$\left(\frac{S}{N}\right)^2 = \int_{-\infty}^{\infty} d\nu \sum_l (2l+1)\frac{P_l^{BH}(\nu)}{P_l^n(\nu)} \ . \qquad (2)$$

Contributions to the S/N are greatest at harmonic degrees l and frequencies ν where the ratio of the numerator in the summation (left panel of Fig. 2) to the denominator (right panel of Fig. 2) is maximized.

A PBH on a radial orbit freely falling from infinity (abbreviated as RFF hereafter) excites solar oscillations with $S/N = 240$ for $m_{BH} = 10^{-10}M_\odot$. This is a conservative estimate for several reasons. Our simulations only last for $t_{sim} = 8$ hours, and thus neglect contributions to the signal from $t > t_{sim}$. However, most of the signal comes from modes with frequencies ν above the acoustic cutoff frequency [15]. These modes are only partially trapped in the solar interior, escaping into the corona on the sound-crossing time $\tau \simeq 2\int dR/c_s = 1.96$ hours, where $c_s(R)$ is the sound speed as a function of solar radius. Simulations with $t_{sim} \gtrsim \tau$ should therefore capture most of the signal. Excluding the core ($R < 0.24\ R_\odot$) from our simulations further reduces the signal, both by neglecting the energy deposited in this region and absorbing waves that reach the inner boundary. This absorbing inner boundary condition removes modes with $\nu \gtrsim 0.2l$ mHz, as can be seen by the dearth of power in this region in the left panel of Fig. 2. The loss of these modes is significant because the noise has very little power in this region as seen in the right panel of Fig. 2. Preliminary simulations with a core radius of 0.1 $R_\odot$ suggest that the true S/N could be greater by a factor of two or more. These arguments imply that $S/N = 240$ is indeed a conservative estimate for $m_{BH} = 10^{-10}M_\odot = 2 \times 10^{23}$ g. Since $S/N \propto m_{BH}$, the minimum detectable PBH ($S/N \sim 1$) on the RFF orbit will have a mass $m_{BH} \simeq 10^{21}$ g.

We have performed simulations with PBHs on three additional orbits: radial infall with a typical Galactocentric velocity of 220 km/s at infinity (RGC), a parabolic orbit that maximizes the time spent at $R < R_\odot$ (MT), and a parabolic orbit that barely skims the solar surface (SS). These orbits are shown in Fig. 3. The S/N for all four simulations as a function of the maximum l included in the summation in Eq. (2) is shown in Fig. 4. Most of the power comes from large scales ($l \lesssim 100$), since modes with higher l are evanescent rather than oscillatory deep in the solar interior where much of the energy is deposited [15]. The small difference between the RFF and RGC simulations, both of which have no angular momentum ($L = 0$), suggests that S/N depends weakly on the orbital energy E. The RFF and MT orbits, both of

which are parabolic ($E = 0$), demonstrate that the S/N depends more strongly on L. Our preliminary simulations with a core radius 0.1 $R_\odot$ suggest an even stronger dependence on L, since the S/N of the RFF simulation doubles while that of the MT simulation remains nearly unchanged. The surface-skimming (SS) orbit has very low S/N, implying that the PBH must penetrate deeply into the solar interior to excite appreciable oscillations.

One of our primary motivations to search for PBHs is the possibility that they constitute the cold dark matter required by cosmology. The Milky Way resides in a dark-matter halo whose local density is approximately $\rho_{DM} \simeq 5 \times 10^{-25}$ g/cm^3 in the solar neighborhood. The Sun orbits the Galactic center with a velocity $v_\odot \simeq 220$ km/s. If PBHs with mass m_{BH} and velocity dispersion $\sigma = v_\odot/\sqrt{2}$ constitute the dark matter, the differential rate at which PBHs with specific energy E and angular momentum L encounter the Sun is [21]

$$\frac{\partial^2 N}{\partial E \partial L} = \frac{2\rho_{DM} L}{m_{BH} v_\odot \sigma} \sqrt{\frac{\pi}{E}} e^{-(2E+v_\odot^2)/2\sigma^2} \sinh\left(\frac{v_\odot \sqrt{2E}}{\sigma^2}\right) . \quad (3)$$

PBHs with $L < L_{\rm max} = \sqrt{2R_\odot(GM + ER_\odot)}$ have pericentric distances less than $R_\odot$, implying that the total rate at which PBHs pass through the Sun is

$$\begin{aligned} N &= \int_0^\infty dE \int_0^{L_{\rm max}} dL \, \frac{\partial^2 N}{\partial E \partial L} , \\ &= \frac{\pi R_\odot^2 \rho_{DM} v_\odot}{m_{BH}} \left[\frac{1}{e\sqrt{\pi}} + \mathrm{erf}(1)\left(\frac{3}{2} + \frac{2GM_\odot}{R_\odot v_\odot^2}\right)\right] , \\ &= 10^{-8}\ \mathrm{yr}^{-1} \left(\frac{\rho_{DM}}{10^{-25}\ \mathrm{g/cm}^3}\right) \left(\frac{m_{BH}}{10^{21}\ \mathrm{g}}\right)^{-1} . \end{aligned} \quad (4)$$

If all PBHs passing through the Sun were detectable, Eq. (4) would provide the event rate of our proposed signal. Since the S/N depends on m_{BH}, E, and L, the true event rate can be found by weighting the integrand with a Heaviside step function that vanishes when the S/N is below a chosen threshold. Unless there is a considerable enhancement in the local PBH density beyond that expected for Galactic dark matter, PBHs are unlikely to be discovered by solar observations alone.

Fortunately, asteroseismologists study oscillations in stars other than our Sun. Such oscillations have been observed by the CoRoT (Convection Rotation and Planetary Transits) [22] and Kepler satellites [23]. Resolution limits these instruments to disk-averaged observations sensitive to only the lowest l. Although this reduces the S/N of each event, the large number of stars that can be continuously monitored could greatly increase the total rate of detectable events. Future missions like the proposed Stellar Imager [24] may even resolve stellar disks, allowing S/N comparable to that for solar events. Further work is needed to establish that PBHs can excite detectable oscillations in stars with structures very different from our Sun. If particle dark matter is not detected directly or discovered at the Large Hadron Collider (LHC), searches for alternative candidates like PBHs must be considered. We believe that asteroseismology might play an important role in these efforts.

Acknowledgements. All calculations were run on the Pleiades supercomputer at NASA Ames Research Center. Many thanks to T. Duvall Jr. for helping to prepare and interpret HMI observations. We are grateful to Tim Sandstrom at NASA Ames for creating impressive pictures of our simulations including Figures 1 and 3. We would like to thank Glennys Farrar, David Hogg, and Andrew MacFadyen for useful conversations. S. M. H. acknowledges support from NASA grant NNX11AB63G.

[1] S. Hawking, Mon. Not. Roy. Astron. Soc. **152**, 75 (1971).
[2] S. W. Hawking, Nature **248**, 30 (1974).
[3] B. J. Carr, S. W. Hawking, Mon. Not. Roy. Astron. Soc. **168**, 399 (1974).
[4] B. J. Carr, Astrophys. J. **201**, 1 (1975).
[5] D. Larson *et al.*, Astrophys. J. Suppl. **192**, 16 (2011).
[6] K. Jedamzik, Phys. Rev. **D55**, 5871 (1997).
[7] D. N. Page, S. W. Hawking, Astrophys. J. **206**, 1 (1976).
[8] P. Sreekumar *et al.* [EGRET Collaboration], Astrophys. J. **494**, 523 (1998).
[9] B. J. Carr *et al.*, Phys. Rev. **D81**, 104019 (2010).
[10] C. Alcock *et al.* [MACHO and EROS Collaborations], Astrophys. J. Lett. **499**, L9 (1998).
[11] P. Tisserand *et al.* [EROS-2 Collaboration], Astron. Astrophys. **469**, 387 (2007).
[12] M. A. Abramowicz *et al.*, Astrophys. J. **705**, 659 (2009).
[13] F. Jansen *et al.*, Astron. Astrophys. **365**, L1 (2001).
[14] G. Peres *et al.*, Astrophys. J. **528**, 537 (2000).
[15] J. Christensen-Dalsgaard, Rev. Mod. Phys. **74**, 1073 (2002).
[16] S. M. Hanasoge *et al.*, Astrophys. J. **648**, 1268 (2006).
[17] S. M. Hanasoge *et al.*, Mon. Not. Roy. Astron. Soc. **391**, 1931 (2008).
[18] R. Wachter *et al.*, Solar Phys., doi:10.1007/s11207-011-9709-6 (2011).
[19] HMI-AIA Joint Science Operations Center, http://jsoc.stanford.edu/.
[20] L. S. Finn, Phys. Rev. D **46**, 5236 (1992).
[21] J. Binney, S. Tremaine, *Galactic Dynamics* (Princeton University Press, Princeton, NJ, 1987).
[22] E. Michel *et al.*, Science **322**, 558 (2008).
[23] W. J. Chaplin *et al.*, Astrophys. J. **713**, L169 (2010).
[24] K. G. Carpenter, C. J. Schrijver, M. Karovska, Astrophys. Space Sci. **320**, 217 (2009).